[5] B. P. Ng, M. H. Er, and C. Kot, "Linear array geometry synthesis with minimum sidelobe level and null control," *Proc. Inst. Elect. Eng.-Microw. Antennas Propag.*, vol. 141, no. 3, pp. 162–166, June 1994.
[6] W. X. Zhang and Y. M. Bo, "Pattern synthesis for linear equal-spaced antenna array using an iterative eigenmodes method," *Proc. Inst. Elect. Eng.*, pt. H., vol. 135, no. 3, pp. 167–170, June 1988.
[7] N. McDonald, "The use of circuit simulators for array-pattern modeling and optimization," *IEEE Antennas Propagat. Mag.*, vol. 42, no. 2, pp. 62–65, April 2000.
[8] M. Chryssomallis, K. Nikolakopoulos, and C. Christodoulou, "Pattern optimization of large array antennas by using only phase control," in *Proc. IEEE AP-S Int. Symp. and USNC/URSI National Radio Science Meeting*, San Antonio, TX, June 17–20, 2002.

A Novel Iterative Solution of the Three Dimensional Electric Field Integral Equation

Conor Brennan, Peter Cullen, and Marissa Condon

***Abstract*—A novel forward backward iterative scheme for solving the three-dimensinoal (3-D) electric field integral equation is presented. This communication details how a naive extension of a 2-D forward backward algorithm to 3-D problems results in convergence difficulties due to spurious edge effects. The method proposed in this communication postulates the use of local "buffer regions" to suppress these unwanted effects and ensure stability. Results are presented illustrating the convergence of the algorithm when applied to scattering by a 15λ square metallic plate with an aperture and a metallic right-angled wedge.**

***Index Terms*—Electric field integral equation (EFIE), iterative methods, method of moments (MoM), scattering.**

I. Introduction

The electric field integral equation (EFIE) offers a full wave formulation to the problem of electromagnetic wave scattering from a perfectly conducting object. However, numerical solution of the EFIE based on the method of moments results in a dense linear system which, for large problems, is impossible to store let alone invert. Instead, iterative solutions are used which do not require the explicit inversion of the matrix but rather sequentially build the solution. Recently there has been much research into what may be termed physically inspired iterative solutions, or informally "current marching" methods. Examples include the method of ordered interactions of [1] and the forward/backward method of [2], both of which were applied to two-dimensional (2-D) problems. A 3-D version was presented in [3] for application to a magnetic field integral equation (MFIE) formulation of a scattering problem. However the MFIE is only applicable to problems involving scattering from closed bodies and one must use the EFIE if one wishes to consider scattering from an open body. This paper presents a current marching algorithm which is applicable to the 3-D EFIE. The algorithm presented constitutes an extension of the ideas presented in [4] in which a similar algorithm is presented for 2-D scattering problems.

Manuscript received September 4, 2003; revised December 23, 2003. This work was supported by the Irish Government/EU through the Enterprise Ireland Informatics Research Initiative under the National Development Plan 2000-2006.

C. Brennan and M. Condon are with RINCE, the School of Electronic Engineering, Dublin City University, Glasnevin, Dublin 9, Ireland (e-mail: brennanc@eeng.dcu.ie).

P. J. Cullen is with the Department of Electrical and Electronic Engineering, Trinity College Dublin, Dublin 2, Ireland.

Digital Object Identifier 10.1109/TAP.2004.834405

II. EFIE

We consider a perfectly conducting scatterer illuminated by a source which induces currents on its surface S. We define the incident electric field $\mathbf{E}^i$ as the field that would exist in the absence of the scatterer. The total field anywhere in space is then given by the sum of the incident and scattered electric fields where the scattered field, $\mathbf{E}^s$, is given by the following integral expression

$$\mathbf{E}^s = -\jmath\omega\mathbf{A} - \nabla\phi \tag{1}$$

where $\mathbf{A}$ and ϕ are the magnetic vector potential and scalar potential, respectively. Applying the requirement of zero tangential fields at a point on the surface of the scatterer results in the EFIE which can be converted to a matrix equation by the introduction of basis functions and a testing procedure [5]. The resultant equation is

$$\mathbf{ZI} = \mathbf{V} \tag{2}$$

where $\mathbf{Z}$ is a dense complex-valued $N \times N$ matrix, where N is the number of basis functions used to discretise the surface current. $\mathbf{V}$ is a vector of size N containing information about the incident field on the scatterer while the vector $\mathbf{I}$ represents the (unknown) amplitudes of the N basis functions. Numerical specification of $\mathbf{I}$ enables us to compute scattered and hence total fields at points in space off the scatterer surface.

III. Forward/Backward Algorithm for 3-D Scatterers

The highly oscillatory nature of the surface current necessitates one to adopt a high sample rate (typically around ten basis functions per wavelength) and means that for problems of practical size it becomes impossible to store, let alone invert, the impedance matrix $\mathbf{Z}$. Instead, the matrix equation is typically solved using an iterative procedure such as the method of conjugate gradients. Recently, there has been much interest in the concept of physically inspired iterative solvers. These solve for the unknown basis function amplitudes $\mathbf{I}$ in a manner that attempts to mimic the physical processes that create the current and can often yield useful results in a reduced number of iterations. Specifically, a current marching algorithm involves decomposing the scatterer into M subregions and "marching" a solution for the current along the scatterer surface from subregion to subregion. The solution at processed subregions is used to set up the problem to be solved at the next subregion, and so on. Mathematically, the algorithm involves decomposing the $\mathbf{Z}$ matrix into blocks, the $\tilde{\mathbf{Z}}_{ij}$ block containing the interactions between basis functions residing in the ith and jth subregions on the scatterer. Each iteration of a forward/backward algorithm involves solving two equations. The first equation is solved for the subregions $i = 1 \ldots M$ in turn and is termed the forward sweep

$$\tilde{\mathbf{Z}}_{ii}\tilde{\mathbf{I}}_i^{(k)} = \tilde{\mathbf{V}}_i - \sum_{j=1}^{i-1}\tilde{\mathbf{Z}}_{ij}\tilde{\mathbf{I}}_j^{(k)} - \sum_{j=i+1}^{M}\tilde{\mathbf{Z}}_{ij}\tilde{\mathbf{I}}_j^{(k-1)} \tag{3}$$

where $\tilde{\mathbf{V}}_i$ and $\tilde{\mathbf{I}}_i$ are the appropriate subvectors of $\mathbf{V}$ and $\mathbf{I}$, respectively. Equation (3) is a matrix equation for the kth estimate of the currents on subregion i. Note that the right-hand side incident fields have been modified by including the effects of the most up to date current estimates available for the other subregions. As it involves a matrix of relatively low order (3) can be efficiently solved using a conjugate gradient solver. The second equation is solved for $i = M \ldots 1$ in turn and corresponds to a backward sweep

$$\tilde{\mathbf{Z}}_{ii}\tilde{\mathbf{I}}_i^{(k+1)} = \tilde{\mathbf{V}}_i - \sum_{j=1}^{i-1}\tilde{\mathbf{Z}}_{ij}\tilde{\mathbf{I}}_j^{(k)} - \sum_{j=i+1}^{M}\tilde{\mathbf{Z}}_{ij}\tilde{\mathbf{I}}_j^{(k+1)}. \tag{4}$$

Again, the right-hand side incident fields have been modified by including the effects of the most up to date current estimates available for

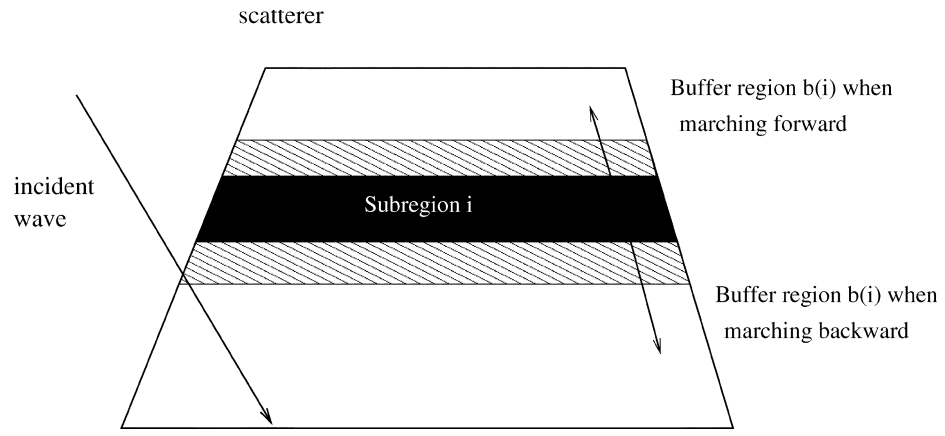

Fig. 1. Subregion (black) along with shaded "buffer regions" to ensure stability of current marching method.

the other subregions. Being of low order (4) can be efficiently solved using a conjugate gradient solver. For the purposes of clarity in discussing the presented numerical results we deem an iteration to be one complete forward sweep followed by a complete backward sweep.

We can examine the convergence or otherwise of the iterative process thus defined by computing how well the governing matrix (2) is satisfied at each iteration. We define the boundary condition percentage error associated with the ith basis function after completion of the nth iteration by[1]

$$e_i^{(n)} = 100.0 \left| \frac{V_i - \sum_{i=1}^{N} Z_{ij} I_j^{(2n)}}{V_i} \right|. \tag{5}$$

The convergence or otherwise of the method can be monitored by computing the average value of this error $\bar{e}^{(n)}$ after each iteration.

Whilst intuitively appealing the iterative process described above fails when applied to a relatively simple 3-D problem. Consider a simple example involving scattering from a metallic square plate of side 2λ centred at (0,0,0) being illuminated by a half-wavelength z oriented dipole located at $(0, -10\sqrt{3}, 10)$ and radiating at 300 MHz. For this example the subregions consisted of six rectangular groupings of basis functions running along the whole width of the plate as schematically shown in Fig. 1. Table I contains the average boundary condition error at each iteration step and illustrates how the iterative method as applied above quickly diverges. To understand the failure of the iterative process as described above we must appreciate that each subregion is effectively considered in isolation when computing the currents on it on any given sweep. Consider the first step in the first forward sweep. The current estimate $\mathbf{I}^{(1)}$ is initialized to zero and (3) reduces to

$$\tilde{\mathbf{Z}}_{11} \tilde{\mathbf{I}}_1^{(1)} = \tilde{\mathbf{V}}_1. \tag{6}$$

Essentially, we are treating subregion one as a physically isolated scatterer. As a consequence, the computed current $\tilde{\mathbf{I}}_1^{(1)}$ will display the singular behavior which characterizes the current at the edges of open-bodied scatterers. While these edge effects are correct and desirable for any edges of the subregion which coincide with the *actual* edges of the entire open-bodied scatterer any edge effects between two interior subregions are undesirable. If the scatterer problem were solved as a whole,

[1]Note that the superscript $(2n)$ is used in the summation because each basis amplitude, I_j, is updated twice during a complete iteration, once during the forward sweep and once during the backward sweep

TABLE I
AVERAGE ERROR AT THE BOUNDARY CONDITION FOR NAIVE FORWARD/BACKWARD APPROACH

Iteration n	Average error $\bar{e}_n$
1	282.7
2	13270.8
3	758249.4
4	43163263.5

no such effects would appear and so it may be concluded that their appearance is due to the artificial decomposition of the scatterer into independently considered subregions and must be suppressed. However, the naive iterative method as suggested by (3) and (4) fails to do this. Consider the next problem to be solved in the initial forward sweep. We have

$$\tilde{\mathbf{Z}}_{22} \tilde{\mathbf{I}}_2^{(1)} = \tilde{\mathbf{V}}_2 - \tilde{\mathbf{Z}}_{21} \tilde{\mathbf{I}}_1^{(1)}. \tag{7}$$

Here, the inaccuracy due to the spurious edge effect on subregion 1 is allowed propagate and distort the computation of $\tilde{\mathbf{I}}_2^{(1)}$. In addition $\tilde{\mathbf{I}}_2^{(1)}$ will also manifest spurious singularity effects on artificial edges within subregion 2.

However we can circumvent this problem quite easily by introducing a certain amount of redundancy into our computations. These extra calculations will be shown to dramatically improve the stability of the iterative process at the small cost of a slightly higher computational burden. We identify for each subregion "buffer regions" (see Fig. 1) which are those areas of the scatterer immediately adjacent to the boundary of the subregion in the direction that we are marching the solution. Note that the definition of the buffer region thus depends on whether we are on the forward or backward sweep of the iterative process. The idea is to include the interactions with the basis functions in this buffer region to suppress the artificial current singularities which, as previously seen, are introduced by the abrupt termination of each subregion. Mathematically this corresponds to replacing the previous forward and backward sweeps with revised versions

$$\tilde{\mathbf{Y}}_{ii} \tilde{\mathbf{J}}_i^{(k)} = \tilde{\mathbf{W}}_i - \sum_{j=1}^{i-1} \tilde{\mathbf{Y}}_{ij} \tilde{\mathbf{I}}_j^{(k)} - \sum_{j>i, j \notin b(i)} \tilde{\mathbf{Y}}_{ij} \tilde{\mathbf{I}}_j^{(k-1)} \tag{8}$$

$$\tilde{\mathbf{Y}}_{ii} \tilde{\mathbf{J}}_i^{(k+1)} = \tilde{\mathbf{W}}_i - \sum_{j<i, j \notin b(i)} \tilde{\mathbf{Y}}_{ij} \tilde{\mathbf{I}}_j^{(k)} - \sum_{j=i+1}^{N} \tilde{\mathbf{Y}}_{ij} \tilde{\mathbf{I}}_j^{(k+1)} \tag{9}$$

where $b(i)$ represents the appropriate buffer region (depending on whether we are marching forward or backward). $\tilde{\mathbf{Y}}_{ii}$ supplements $\tilde{\mathbf{Z}}_{ii}$

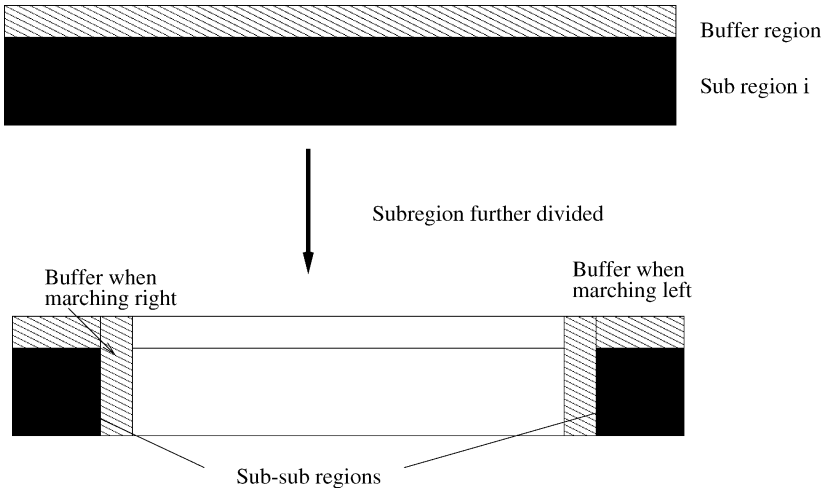

Fig. 2. Subregion i can be further subdivided facilitating efficient current marching solution of (8) and (9).

with information about the interaction between basis functions in i and those in the appropriate (forward or backward) buffer region

$$\tilde{\mathbf{Y}}_{ii} = \begin{bmatrix} \tilde{\mathbf{Z}}_{ii} & \tilde{\mathbf{Z}}_{ib(i)} \\ \tilde{\mathbf{Z}}_{b(i)i} & \tilde{\mathbf{Z}}_{b(i)b(i)} \end{bmatrix} \tag{10}$$

while $\tilde{\mathbf{Y}}_{ij}$ supplements $\tilde{\mathbf{Z}}_{ij}$ with information about the interaction between basis functions in j and those in the appropriate buffer region

$$\tilde{\mathbf{Y}}_{ij} = \begin{bmatrix} \tilde{\mathbf{Z}}_{ij} \\ \tilde{\mathbf{Z}}_{b(i)j} \end{bmatrix} \tag{11}$$

$\tilde{\mathbf{J}}_i^{(k)}$ and $\tilde{\mathbf{W}}_i$ are given by

$$\tilde{\mathbf{J}}_i^{(k)} = \begin{bmatrix} \tilde{\mathbf{I}}_i^{(k)} \\ \tilde{\mathbf{I}}_{b(i)} \end{bmatrix} \tag{12}$$

$$\tilde{\mathbf{W}}_i = \begin{bmatrix} \tilde{\mathbf{V}}_i \\ \tilde{\mathbf{V}}_{b(i)} \end{bmatrix}. \tag{13}$$

This modification ensures that local information from basis functions in the buffer region suppresses any spurious edge effect that would otherwise be present. Computationally it is a little more cumbersome to solve (8) and (9) due to the fact that the matrices are of higher order. The currents calculated in the buffer region $\tilde{\mathbf{I}}_{b(i)}$ are redundant in the sense that they are only computed to keep the currents in subregion i under control. They are overwritten on moving to the next subregion. However in practice the buffer region is quite small and the increased computational overhead is offset by the rapid convergence of the algorithm.

A. Recursive Algorithm

Initial implementations of the algorithm proceeded by breaking a scatterer into rectangular groups of basis functions which spanned the whole width of the scatterer as illustrated in Fig. 1. However, with this approach, as the scatterer size increases the size of each subregion grows accordingly. When one adds in the extra computational burden imposed by the buffer region interactions the solution of the matrix (8) and (9) quickly becomes quite onerous. However, it is possible to recursively apply the ideas presented in the previous section to enable the efficient solution of these equations also. As depicted in Fig. 2 each subregion can in turn be further subdivided into smaller subsubregions and the matrix (8) and (9) are solved by marching currents back and forth within subregion i and its buffer. Essentially, the scattering problem is solved by a process of forward and backward sweeps, where the local problems within each forward/backward sweep are solved by a process of sweeping left and right. Again care must be taken to define suitable buffer regions to suppress unwanted edge effects.

IV. Results

The techniques described in this paper have been applied to a number of problems. The first example involves a right angled finite wedge composed of two perfectly conducting plates of side 2λ meeting along a common edge. The first plate is centred at (0, 0, 0) while the second is centred at (0, 1, 1) The source is a half-wave dipole located at $(0, -10\sqrt{3}, 10)$ and radiates at 300 MHz. Each plate was subdivided into 6 rectangular subregions each of which spanned the width of the plate. The currents were then marched forward and backward along the wedge structure. The scattered fields along a straight line running from $(1.5, -20, 10)$ to (1.5, 20, 10) were calculated after each iteration and are plotted in Fig. 3. We note the rapid convergence of the scattered fields, the solution after 3 iterations being essentially identical to a reference solution obtained using a conjugate gradient method. The forward backward method took 92 min to perform three forward backward sweeps running on a 1.6 GHz PC. A conjugate gradient solver took 3.46 h to reach the same degree of accuracy. The algorithm was also applied to a larger finite right angled wedge with sides equal to 5λ. Again rapid convergence was observed with the average boundary error falling to 6% after only three iterations. The second example involves scattering from a metallic square plate of side 5m centred at the point (0, 0, 0) containing a square aperture of side 1λ centred at $(-2, -2, 0)$. The plate is illuminated by a dipole located at $(0, -10\sqrt{3}, 10)$ this time radiating at 900 MHz. For the purpose of applying the algorithm the plate was subdivided into 10 rectangular subregions each of which spanned the width of the plate. The currents were then marched forward and backward along the plate surface. For this example the currents within each subregion were obtained by marching left/right once, as described in Section III-A. At this level each subsubregion (see Fig. 2) was a square section of plate of side 1.5λ. The buffer zone was such that the entire computational region for each subsubproblem was a square of size 2λ. Table II shows the average boundary condition error versus the iteration number. The computation time needed to yield an average error of under 2% was 30 h, under a quarter of the time needed by a conjugate gradient solver to reach a similar level of convergence. While this represents a significant saving this computation time is still quite large. However, it should be noted that the computation time could be reduced further by suitably preprocessing the problem. This would involve identifying the

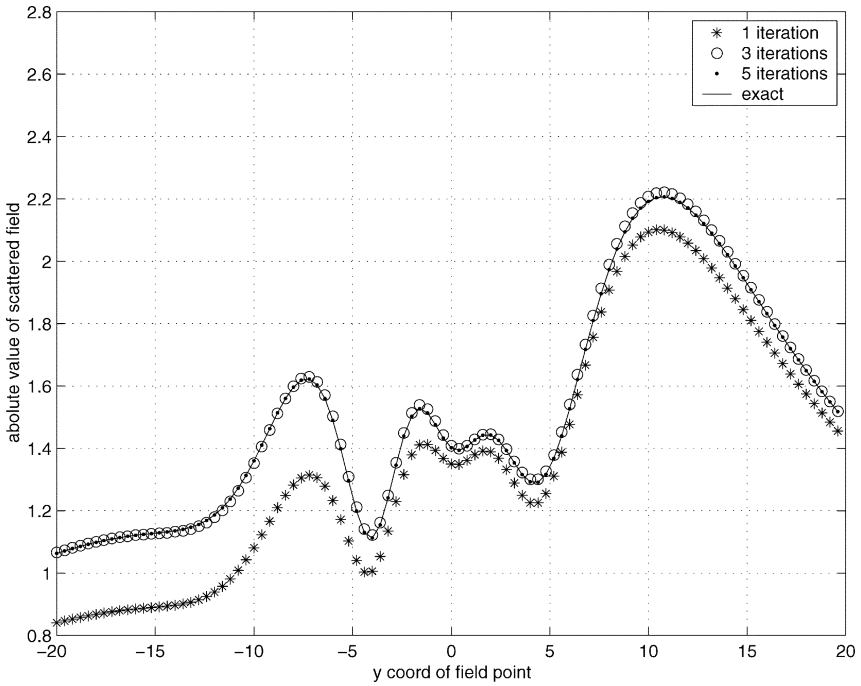

Fig. 3. Convergence of scattered fields over wedge.

TABLE II
AVERAGE ERROR AT THE BOUNDARY CONDITION AS A FUNCTION OF ITERATION NUMBER FOR EXAMPLE TWO

Iteration n	Average error
1	13.6146
2	2.27561
3	0.42557

subregions along with their buffer zones in advance and then creating and inverting the local impedance matrices. These inverted matrices could be stored in memory and used to efficiently solve the appropriate matrix problems as we sweep through the structure. A further saving could be had by implementing an appropriate acceleration method such as the fast far field algorithm [6] to expedite interactions between far-away sections of scatterer. These improvements will form the basis of future work.

This paper has shown that a forward-backward scheme is possible for 3-D scattering problems described by the EFIE. Numerical examples have demonstrated the applicability of the method. However, further work needs to be done to assess the optimal application of this method. In particular the question of how to choose the size of the buffer regions needed to guarantee stability for a more general problem involving an imperfectly conducting body with a more general geometry must be addressed. It is felt that the work presented here will start as a useful starting point to answer these questions.

V. CONCLUSION

This paper has presented a modified forward/backward algorithm for iteratively solving the 3-D EFIE. Stability was achieved by the adoption of buffer regions which suppress spurious edge effects which would otherwise grow to dominate the solution. Results were provided showing the application of the algorithm to some problems. Future work will see the incorporation of suitable acceleration methods and the extension to imperfectly conducting bodies of more general shape.

REFERENCES

[1] Kapp and Brown, "A new numerical method for rough-surface scattering calculations," *IEEE Trans. Antennas Propagat.*, vol. 44, pp. 711–721, May 1996.
[2] D. Holliday *et al.*, "Forward-backward: A new method for computing low-grazing angle scattering," *IEEE Trans. Antennas Propagat.*, vol. 44, pp. 722–729, May 1996.
[3] Zaphorets and Levy, "Current marching technique for electromagnetic scattering computations," *IEEE Trans. Antennas Propagat.*, vol. 47, pp. 1016–1024, 1999.
[4] D. Torrungrueng and E. Newman, "The multiple sweep method of moments (MSMM) analysis of electrically large bodies," *IEEE Trans. Antennas Propagat.*, vol. 45, pp. 1252–1258, Aug. 1997.
[5] S. M. Rao, D. R. Wilton, and A. W. Glisson, "Electromagnetic scattering by surfaces of arbitrary shape," *IEEE Trans. Antennas Propagat.*, vol. AP-30, pp. 409–418, May 1982.
[6] A. McCowen, "Efficient 3-D moment-method analysis for reflector antennas using a far-field approximation technique," *Proc. Inst. Elect. Eng. Proc. Micro. Ant. Prop.*, vol. 146, no. 1, pp. 7–12, Feb. 1999.